Acta Pharmaceutica Sinica B 2025;15(11):6019−6033

Chinese Pharmaceutical Association
Institute of Materia Medica, Chinese Academy of Medical Sciences

Acta Pharmaceutica Sinica B

www.elsevier.com/locate/apsb
www.sciencedirect.com

ORIGINAL ARTICLE

Engineered *Escherichia coli Nissle* 1917 targeted delivery of extracellular PD-L1-mFc fragment for treating inflammatory bowel disease

Yuhong Wang[a,†], Lin Hu[b,*,†], Lei Wang[c,†], Chonghai Zhang[b], Wenhao Shen[b], Hongli Yang[a], Min Li[c], Xin Zhang[d,e], Mengmeng Xu[f], Muxing Zhang[g,*], Kai Yang[a,b], Xiaopeng Tian[d,e,*]

[a]*Department of Pathology, The First Affiliated Hospital of Soochow University, Suzhou 215000, China*
[b]*State Key Laboratory of Radiation Medicine and Protection, School of Radiation Medicine and Protection & School for Radiological and Interdisciplinary Sciences (RAD-X), Collaborative Innovation Center of Radiation Medicine of Jiangsu Higher Education Institutions, Soochow University, Suzhou 215123, China*
[c]*Institute of Biology and Medical Sciences, Soochow University, Suzhou 215123, China*
[d]*National Clinical Research Center for Hematologic Diseases, Jiangsu Institute of Hematology, The First Affiliated Hospital of Soochow University, Suzhou 215000, China*
[e]*Institute of Blood and Marrow Transplantation, Collaborative Innovation Center of Hematology, Soochow University, Suzhou 215000, China*
[f]*Department of Pathology, The Second Affiliated Hospital of Soochow University, Suzhou 215004, China*
[g]*Department of Clinical Nutrition, The First Affiliated Hospital of Soochow University, Suzhou 215000, China*

Received 20 December 2024; received in revised form 24 February 2025; accepted 20 April 2025

KEY WORDS

Escherichia coli Nissle 1917;
Inflammatory bowel disease;
Protein delivery;
T cell;
Programmed cell death ligand 1;

Abstract Inflammatory bowel disease (IBD) is an autoimmune disorder involving complex immune regulation, where balancing localized and systemic immunosuppression is a key challenge. This study aimed to enhance the therapeutic efficacy by engineering the probiotic *Escherichia coli Nissle* 1917 (EcN). We removed endogenous plasmids pMUT1 and pMUT2 from wild-type EcN and expressed the mPD-L1 (19−238 aa)-mFc fusion protein on the bacterial surface using a cytolysin A (ClyA) fragment. This modification stabilized mPD-L1 (19−238 aa) protein expression and promoted its recruitment to outer membrane vesicles (OMVs). The engineered strain, EcN$\Delta_{pMUT1/2}$-ClyA-mPD-L1-mFc (EcN-ePD-L1-mFc), features conditional ePD-L1-mFc expression under the araBAD promoter, enhancing gut-targeted release and reducing systemic side effects. This strain improved treatment targeting and

*Corresponding authors.
E-mail addresses: hulin@suda.edu.cn (Lin Hu), zmxnutrition@163.com (Muxing Zhang), txpchina@163.com (Xiaopeng Tian).
[†]These authors made equal contributions to this work.

Peer review under the responsibility of Chinese Pharmaceutical Association and Institute of Materia Medica, Chinese Academy of Medical Sciences.

https://doi.org/10.1016/j.apsb.2025.08.002

Outer membrane vesicles;
Targeted local therapy;
Gut microbes

efficiency by enabling direct ePD-L1-mFc interaction with immune cells at inflammation sites. OMVs from this strain induced Treg proliferation, inhibited effector T cell proliferation *in vitro*, and significantly improved intestinal inflammation and colonic epithelial barrier repair *in vivo*. Additionally, the bacterium restored intestinal microbiota balance, increasing Lactobacillaceae and reducing *Bacteroides*. This study highlights the engineered bacterium's potential for targeted intestinal immune modulation and offers a novel local IBD treatment approach with promising clinical prospects.

1. Introduction

Inflammatory bowel disease (IBD) is a chronic gastrointestinal disorder that includes Crohn's disease and ulcerative colitis (UC) and affects the gastrointestinal tract and colon, respectively. IBD is the result of a complex interplay between genetic susceptibility, immune regulation, and intestinal microbiota[1,2]. Immune imbalances due to the overactivation of T helper cells (Th cells) and the excessive production of pro-inflammatory mediators drive the onset and progression of IBD[3].

Current therapeutic options for IBD include 5-aminosalicylic acid, glucocorticoids, immunosuppressants (methotrexate and thiopurine), and small-molecule drugs and biologics[4]. Small-molecule drugs include selective Janus kinase inhibitors[5-7], sphingosine-1-phosphate receptor modulators[8], oral *SMAD7* antisense oligonucleotides[9,10], and phosphodiesterase-4 inhibitors[11,12]. These drugs are useful for treating IBD because of their convenient administration, rapid metabolism, and non-immunogenicity. For instance, JAK inhibitors have been shown to inhibit pro-inflammatory cytokine signaling pathways, significantly reducing inflammation in IBD patients. However, while small-molecule drugs offer advantages such as a favorable pharmacokinetic profile, they do not always provide sustained efficacy in the long term due to issues like drug resistance and the potential for developing side effects. Additionally, some biologics, including interleukin IL-12, IL-23 and integrin inhibitors[13-15], have markedly improved therapeutic outcomes. However, despite their efficacy, biologics are not without their challenges. They are associated with a risk of infusion reactions, immunogenicity (leading to the development of anti-drug antibodies), and, in some cases, an increased risk of malignancies, especially in long-term use. Furthermore, the high cost and the need for administration in a healthcare setting limit the widespread use of these therapies. In light of these issues, novel strategies such as engineered bacteria are being explored to offer a more targeted, personalized, and potentially safer approach to IBD treatment.

IBD treatment is based primarily on pharmacological therapies to reduce gut inflammation. Probiotics are a promising treatment option because of their ability to modulate the intestinal microbiota, enhance intestinal barrier function, and improve immune responses. Further, oral probiotics can mitigate drug side effects[16]. Among the 45 preclinical studies of engineered probiotics reviewed, 11 strains were genetically modified to produce therapeutic substances, including IL-10, antimicrobial peptides, antioxidant enzymes, and short-chain fatty acids, all of which showed potential efficacy in treating colitis. Based on these findings, one engineered probiotic, IL-10-producing *Lactococcus lactis*, was selected for a clinical trial involving 10 patients with Crohn's disease. The trial demonstrated that this engineered strain was safe and led to a reduction in disease activity among the patients. However, despite these promising results, *Lactococcus lactis* is not yet approved for clinical use[17]. *Escherichia coli* Nissle 1917 (EcN) supports intestinal health by suppressing the growth of pathogenic bacteria, modulating immune factors, and strengthening mucosal barrier integrity. Clinical trials have reported significant improvements in the clinical activity index (CAI) of ulcerative colitis (UC) patients, along with reductions in inflammatory markers such as C-reactive protein and fecal calprotectin[18]. The efficacy of this strain in maintaining UC remission is similar to that of mesalazine[19]. However, EcN has limited ability to colonize the gastrointestinal tract[20], underscoring the need to enhance its efficacy through genetic engineering.

The programmed death 1 (PD-1) pathway, including the PD-1 ligands PD-L1 and PD-L2, is critical in regulating immune tolerance and autoimmune responses, particularly in chronic infections and cancers, by inhibiting T cell activation[21-23]. PD-1^+ and PD-$L1^+$ lymphocytes are strongly upregulated in the lamina propria of IBD patients, especially in UC patients, suggesting that the PD-1/PD-L1 pathway plays a role in the pathogenesis of UC[24,25]. In animal models of chronic UC, the high expression of PD-L1 plays a crucial role in the aberrant regulation of $CD4^+$ and $CD8^+$ effector T cells, leading to intestinal microbiota dysregulation[26,27]. Blocking the PD-1/PD-L1 pathway can result in colonic inflammation, while PD-L1 alleviates the symptoms of enteritis in mice with dextran sulfate sodium (DSS)-induced UC[28-30]. Furthermore, the PD-1 inhibitor nivolumab and the PD-L1 inhibitor atezolizumab can induce immune-related UC[31]. Therefore, PD-L1 is a promising treatment for IBD. However, given its strong immunosuppressive effects, the systemic administration of PD-L1 may increase the risk of infections and cancer, necessitating the development of more precise drug delivery systems.

Outer membrane vesicles (OMVs) are non-replicating particles naturally secreted by Gram-negative bacteria and can serve as carriers of therapeutic components because of the particulate nature and good biocompatibility of these vesicles. OMVs contain pathogen-associated molecular patterns and thus can function as immune stimulators and nano-pathogenoids[32,33]. For instance, an OMV-based meningococcal vaccine reduced the incidence and mortality of meningitis in New Zealand[34]. Moreover, homologous or heterologous antigens from different pathogens or sources can be incorporated into OMVs by genetic engineering[35]. For instance, *E. coli*-derived OMVs expressing antigens from the influenza virus and *Plasmodium falciparum* can stimulate the production of specific antibodies against these pathogens[36,37]. These results prove that homologous or heterologous antigens can be attached to OMVs, effectively serving as molecular carriers.

Herein, we excised the endogenous plasmids pMUT1 and pMUT2 from wild-type EcN and expressed the PD-L1 (19−238

aa)-mFc fusion protein on the bacterial surface using a cytolysin A (ClyA) fragment. This modification stabilized the protein expression of mPD-L1 (19−238 aa) and increased its deployment in OMVs. This approach allowed producing a novel bacterial strain, EcN$\Delta_{pMUT1/2}$-ClyA-mPD-L1-mFc (EcN-ePD-L1-mFc). Furthermore, the L-arabinose-inducible araBAD promoter enabled the conditional expression of ePD-L1-mFc, increasing its release into the intestine, reducing systemic side effects and improving treatment safety and efficacy. This engineered strain significantly enhanced treatment targeting and efficacy through the direct interaction of ePD-L1-mFc on OMVs with immune cells at sites of intestinal inflammation. The ePD-L1-mFc-expressing EcN strain attenuated enteritis by improving intestinal barrier function *in vitro* and *in vivo*. Further, this strain recovered the intestinal levels of short-chain fatty acids (SCFAs) by increasing the relative abundance of Lactobacillaceae and decreasing the abundance of *Bacteroides* (Fig. 1). These results underscore the clinical applicability of this engineered bacterial strain in modulating intestinal immunity and introduce a novel therapeutic approach for the local treatment of IBD.

2. Materials and methods

2.1. Materials

Dulbecco's modified Eagle's medium with high glucose (DMEM) (Punosai Biotechnology Co., Ltd., FM50210, Wuhan, China), fetal bovine serum (Novizan Biotechnology Co., Ltd., F101-03, Nanjing, China), 100 × penicillin−streptomycin solution (Xinsaimei Biotechnology Co., Ltd., C100C5, Suzhou, China), L-arabinose (Aladdin Biotechnologies, A106195-100g, Shanghai, China), TieChui *E. coli* Lysis Buffer (Boyi Biological Technology Co., Ltd., BR0005-02/BR0005-03, Changzhou, China), 4′,6-diamidino-2-phenylindole (DAPI) (Sikejie Biotechnology Co., Ltd., EE0015, Shandong, China), cell culture plates (Sening Biotechnology Co., Ltd., 1022000, Hangzhou, China), 96-well plates (Sening Biotechnology Co., Ltd., 1014000), ampicillin (Target Molecule Corp., T0814L-200 mg, Boston, MA, USA), Cyanine5.5 (Cy5.5) (MedChem Express, HY-D0924, Shanghai, China), and rabbit polyclonal anti-FLAG tag antibody (Proteintech, 20543-1-AP, Wuhan, China).

Environmentally friendly dewaxing transparent liquid (G1128), 20 × citric acid antigen retrieval solution (pH 6.0) (G1202), 20 × Tris-EDTA antigen retrieval solution (pH 9.0) (G1203), 20 × Tris-EDTA antigen retrieval solution (pH 8.0) (G1206), DAB chromogenic solution (G1212), and hematoxylin (G1004) were purchased from Wuhan Saiwei Biotechnology Co., Ltd.

The primary antibodies used in flow cytometry, Western blotting, and immunohistochemistry are listed in Supporting Information Table S1.

2.2. Animal rearing

Female C57BL/6 mice (6−8 weeks) (Weitong Lihua Experimental Animal Technology Co., Ltd., Beijing, China) were housed in an animal facility in individually ventilated cages with 5 mice per cage at 20−22 °C and relative humidity of 30%−70% under a 12 h light/12 h dark cycle. Food and water were supplied ad libitum. All animal experiments received approval from the Animal Ethics Committee at Soochow University (Suzhou, China, No. 202307A0124) and were conducted following the prescribed guidelines for animal use in scientific research.

2.3. Construction of EcN$\Delta_{pMUT1/2}$

To create the engineered strain EcN$\Delta_{pMUT1/2}$, we deleted the endogenous plasmids pMUT1 and pMUT2 from the wild-type *Escherichia coli* Nissle 1917 (EcN) strain *via* the CRISPR-Cas9 System[38]. Initially, we constructed guide plasmids pTargetF1 and pTargetF2 to target pMUT1 and pMUT2, respectively. The targeting sgRNA was integrated *via* reverse PCR using overlapping primers, each containing a specific 20-base pair gRNA target sequence. The guide plasmids were assembled using the

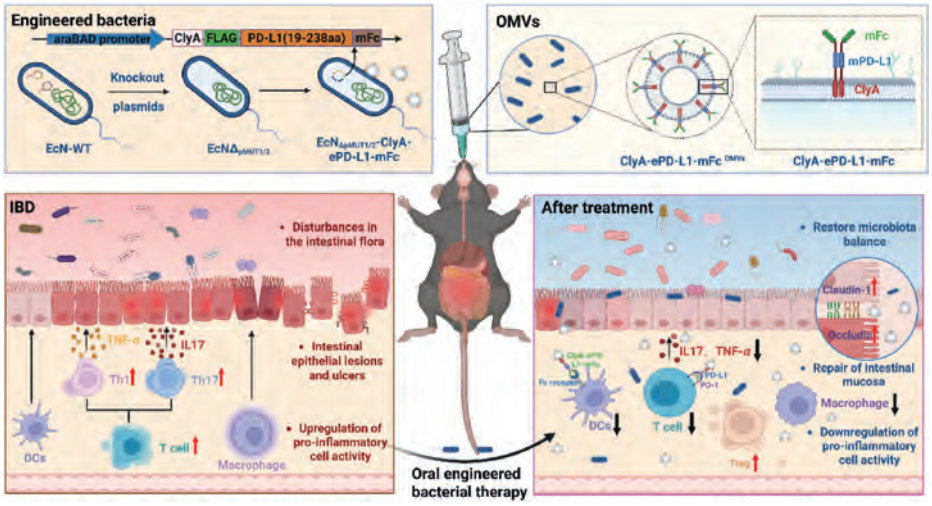

Figure 1 Bioengineered bacterial strain EcN-ePD-L1-mFc used in the local treatment of inflammatory bowel disease in mice. The endogenous plasmids pMUT1 and pMUT2 were removed from wild-type *Escherichia coli* Nissle 1917 (EcN) by genetic engineering to produce EcN$\Delta_{pMUT1/2}$ and improve recombinant protein expression. The ClyA-PD-L1-mFc fragment was transfected into EcN to create EcN$\Delta_{pMUT1/2}$-ClyA-PD-L1-mFc (EcN-ePD-L1-mFc). The secretion of outer membrane vesicles (OMVs) by arabinose-induced EcN-ePD-L1-mFc in the intestinal tract alleviates inflammatory bowel disease by inhibiting immune cell activity and cytokine secretion and restoring the intestinal flora.

Ready-to-Use Seamless Cloning Kit (Sangon Biotechnology, No. B632219, Shanghai, China) following inverse PCR and subsequently transformed into DH5α competent cells (Sangon Biotechnology, No. B528413). Sequencing confirmed the integration of the N20 guide region in the plasmids, and pTargetF1 and pTargetF2 were extracted for further use. Next, we utilized CRISPR/Cas9 for genome editing. The pCas plasmid was electroporated into EcN, and positive colonies were selected through PCR identification and culture on LB kan^+ plates (50 μg/mL). Subsequently, 100 ng of pTargetF1 was electroporated into these bacteria, and clones were selected on LB Kan^+ Spectinomycin plates, resulting in the strain EcN (pCas, ΔpMUT1, pTargetF1) as confirmed by PCR screening. The screened strains were induced with IPTG to eliminate the pTargetF1 plasmid, and clones were selected on LB Kan^+ plates. After PCR identification and screening, we obtained the strain EcN (pCas, ΔpMUT1). Using the same methodology, we electroporated 100 ng of pTargetF2 into the bacteria and subsequently eliminated pTargetF2 to obtain EcN (pCas, ΔpMUT1, ΔpMUT2). Finally, the EcN (pCas, ΔpMUT1, ΔpMUT2) strain was cultured overnight at 37 °C on LB plates without antibiotics until the optical density (OD) at 600 nm reached 0.6−0.9, followed by inoculation onto fresh LB plates without antibiotics. Colonies were selected and subcultured on LB Kan^+ plates. The clones sensitive to kanamycin were identified as having eliminated pCas, resulting in the final strain $EcN\Delta_{pMUT1/2}$. The excision of *pMUT1* and *pMUT2* was confirmed by agarose gel electrophoresis. PCR amplification products were mixed with 6 × loading buffer and loaded onto a 1.5% agarose gel. Electrophoresis was conducted at 100 V in 1 × TAE buffer for 45 min. DNA was visualized by ethidium bromide staining. The presence and size of target DNA fragments were analyzed using an ultraviolet transilluminator. The primer sequences are shown in Supporting Information Table S2.

2.4. pBAD-ClyA-PD-L1 (19−238 aa)-mFc plasmid construction and bacterial culture

The *ClyA-PD-L1 (19−238 aa)-mFc* gene was cloned between the NcoI and HindIII restriction sites of the pBAD vector containing the L-arabinose-inducible araBAD promoter and ara-C regulator. The plasmid sequence is shown in Supporting Information Table S3. We fused the extracellular fragment of mouse PD-L1 (amino acids 19−238) to the C-terminus of the bacterial outer membrane protein ClyA, with a Flag tag inserted between them. The Fc fragment of mouse *IgA* was then attached to the C-terminus of PD-L1. Then, the expression plasmid pBAD-ClyA-PD-L1 (19−238 aa)-mFc was transfected into $EcN\Delta_{pMUT1/2}$ to produce the recombinant strain $EcN\Delta_{pMUT1/2}$-ClyA-PD-L1 (19−238 aa)-mFc (EcN-ePD-L1-mFc). This strain was grown in LB medium supplemented with ampicillin (50 μg/mL) at 37 °C and 220 rpm for 12 h until the optical density (OD) at 600 nm reached 0.6−0.9.

2.5. Analysis of protein expression

The pBAD-mBaoJin plasmid was electroporated with wild-type EcN and $EcN\Delta_{pMUT1/2}$ with a voltage of 2.5 kV, a resistance of 200 Ω, a time constant of 5 ms, and three electroporations. The strains expressing GFP green fluorescent protein were obtained and named EcN-WT-GFP and $EcN\Delta p_{MUT1/2}$-GFP, respectively. Cultures were grown in LB medium at 37 °C with shaking at 220 rpm for 24 h. Kanamycin (50 μg/mL) was added. Fluorescence imaging was performed using an *in vivo* imaging system. Wild-type EcN and $EcN\Delta_{pMUT1/2}$ were lysed using TieChui *E. coli* Lysis Buffer (Changzhou Boyi Biotechnology Co., Ltd., BR0005-02, Changzhou, China), and total protein was extracted according to the manufacturer's instructions. Protein concentration was determined using the BCA protein assay kit (Novizan Biotechnology Co., Ltd., E112-02, Nanjing, China). Protein lysates (30 μg) were separated by SDS-PAGE and transferred to a polyvinylidene fluoride membrane. The membrane was blocked with 5% skim milk (Sangon Biotech; A600669-0250) and incubated with an anti-Myc monoclonal antibody. Proteins were detected using enhanced chemiluminescent reagents (Bio-Rad, 1705061, Hercules, CA, USA). Fluorescence intensity was quantified using ImageJ software (version 1.8.0; National Institutes of Health, Bethesda, MD, USA).

2.6. Preparation and characterization of OMVs

When the optical density (OD_{600}) of EcN, EcN-ePDL1, and EcN-ePDL1-mFc cultures reached 0.6−0.8, 0.2% arabinose was added to the culture to induce protein expression, and then incubated at 37 °C for 6 h. The culture was centrifuged at 4 °C and 1700×*g* (Eppendorf, Centrifuge 5702 R/RH−FastTemp, Hamburg, Germany) for 20 min, and the supernatant was filtered through a 0.22 μm filter (Wuxi Naes Biotechnology Co., Ltd., No. 343011, Wuxi, China) under vacuum. The filtrate was concentrated to 50 mL using a 50 kDa ultrafiltration membrane (Millipore, UFC905008, Billerica, MA, USA) and a 0.22 μm disposable syringe filter. OMVs were resuspended in 1 mL of PBS, centrifuged at 150,000×*g* (Beckman Coulter, L 90K Ultracentrifuge, Model 80XP XE, Brea, CA, USA) for 3 h at 4 °C, and stored at −20 °C. OMVs were extracted from $EcN\Delta_{pMUT1/2}$ using the same protocol, and bacteria were grown under identical conditions for 18 h. The concentration of exosomal proteins was quantified using a BCA protein assay kit (Novizan Biotechnology Co., Ltd., E112-02, Nanjing, China). The shape of OMVs was analyzed by transmission electron microscopy (TEM) (Tecnai G2 Spirit BioTwin, FEI, Eindhoven, The Netherlands). The size distribution and zeta potential of OMVs were evaluated by dynamic light scattering (DLS) using a Zetasizer Nano ZS90 (Malvern Instruments Ltd., Zetasizer Nano ZS90, Malvern, Worcestershire, UK).

2.7. Western blotting

Heterologous protein expression in engineered bacteria and OMVs was analyzed by western blotting. Total protein was extracted from bacteria using a bacterial protein extraction kit (Puyihua Technology Co., Ltd., C600596, Beijing, China) following the manufacturer's instructions. Proteins from OMVs were mixed with the exosome solution at a 4:1 ratio using a 5 × loading buffer and heated at 100 °C for 15 min. Protein lysates (30 μg per sample) were subjected to SDS-PAGE and transferred onto a polyvinylidene fluoride membrane. The membrane was blocked with 5% skim milk (Sangon Biotech, A600669-0250, Shanghai, China) and incubated with rabbit polyclonal anti-WO tag antibody (Sanying Biotechnology Co., Ltd., 20543-1-AP, Wuhan, China) and secondary antibodies. Immunoreactive bands were visualized using an enhanced chemiluminescence system (Bio-Rad, 1705061, Hercules, CA, USA). Fluorescence intensity was quantified using ImageJ software version 1.8.0.

2.8. Intestinal residency

C57BL/6 mice (12 in each group) were randomly divided into 2 groups to evaluate the intestinal retention ability of transgenic bacteria. Each mouse was gavaged with 200 μL of a solution containing Cy5.5-labeled $EcN\Delta_{pMUT1/2}$ or EcN-ePD-L1-mFc (1.0×10^{13} CFU/mL). Mice were euthanized at four-time points (3, 6, 12, and 24 h; three mice per time point), and gastrointestinal images were acquired using an *in vivo* imaging system to assess the retention of engineered bacteria.

2.9. Epithelial penetration assay

Healthy C57BL/6 mice were selected for 6−8 weeks, and epithelial osmosis was performed after a 6 h fasting period. Anesthetize the mouse with 0.5%−1.0% isoflurane and perform intestinal ligation. $EcN\Delta_{pMUT1/2}^{OMV}$ (50 μg) and EcN-ePDL1-mFc^{OMVs} (50 μg) were injected into the ligated segments. Two hours later, these segments were excised for immunofluorescence analysis. Cell nuclei were stained with DAPI (blue), and OMVs were labeled with an anti-PD-L1 antibody (green).

2.10. Presentation of OMVs to murine dendritic cells (DCs) in vitro

Coverslips were washed with absolute ethanol and rinsed three times with sterile PBS. The coverslips were placed in 12-well plates, and 2 mL of DMEM complete medium containing 10% fetal bovine serum and 1% streptomycin was added. Approximately 4.0×10^5 cells were seeded per well in these plates and incubated at 37 °C with 5% CO_2 for 24 h until 80% confluence. Then, 100 μL of a solution containing Cy5.5-labeled $EcN\Delta_{pMUT1/2}^{OMV}$ (50 μg) and EcN-ePDL1-mFc^{OMVs} (0.5 μg/μL) was added, and cells were incubated under the same conditions for 5, 15, 30, 60, and 120 min. After each incubation, the medium was discarded, and cells were washed with PBS three times (5 min each). Cells were fixed with 4% paraformaldehyde for 30 min and washed with PBS three times. The coverslips were blocked with 5% bovine serum albumin for 1 h, washed three times with PBST, and mounted with Vectashield mounting medium containing DAPI (Vector Laboratories, Birmingham, CA, USA). Cells were imaged on a scanning laser confocal microscope (Nikon Corporation, Confocal Microscope, Model A1, Tokyo, Japan).

2.11. Inhibition of immune cell function by OMVs in vitro

In each well of a 96-well plate, 100 μL of a mixture containing anti-CD3 (BD Biosciences, 553238, Franklin Lakes, New Jersey, USA) (2 μg/mL), anti-CD28 (BD Biosciences, 553295) (0.4 μg/mL) was added. The plates were sealed and stored at 4 °C overnight. Spleen cells from C57BL/6 mice were mechanically dissociated, filtered, and resuspended at a concentration of 5.0×10^5 cells/mL. PBS, $EcN\Delta_{pMUT1/2}^{OMVs}$ and EcN-ePD-L1-mFc^{OMVs} (50 μL each) were added to the wells and analyzed by flow cytometry (five wells per group). The streaming data was analyzed by NovoExpress software (NovoCyte, NovoExpress Software, Palo Alto, CA, USA), and the histograms were analyzed by GraphPad Prism 8 with a *t*-test.

2.12. Evaluation of the effect of engineered bacteria on IBD

Twenty-five healthy C57BL/6 female mice (20 g) were housed in a specific pathogen-free environment. The animals were randomly assigned to receive 2% DSS (*w*/*v*) (groups 2 to 5) or PBS (control group), with five animals per group. The experimental groups were gavaged with DSS (group 2), $EcN\Delta_{pMUT1/2}$ (group 3), EcN-ePD-L1-mFc (group 4), or EcN-ePD-L1-mFc + 2% arabinose (group 5) (1.0×10^9 CFUs) on Days 0, 3, 6 and 9. Group 5 received 0.2% arabinose for 12 h daily post-gavage to induce protein expression. On Day 12, the mice were euthanized, the weight was recorded, and blood was collected *via* enucleation. Blood samples from all mice were centrifuged at $1000\times g$ (Eppendorf, Centrifuge 5702 R/RH−FastTemp) at room temperature for 1 h, and the supernatant was stored at −80 °C for cytokine analysis. Mesenteric lymph nodes were harvested and immersed in 1640 medium to assess immune cell maturity. The gastrointestinal tract (cecum to anus) was extracted and individually stored in centrifuge tubes. Then, colonic segments were excised, suspended in 1640 medium for hematoxylin−eosin (H&E) staining, paraffin sectioning, and flow cytometry analysis. The spleen and liver were weighed and stored. Heart, lung, and kidney tissues were collected for H&E staining. Cecal contents were collected and used for 16S rRNA gene sequencing and quantification of the levels of SCFAs.

2.13. H&E staining

Tissue samples from the animals were collected, fixed in a 4% paraformaldehyde solution, and then processed for paraffin embedding. The paraffin-embedded tissues were sectioned into 7 μm thin slices and placed in an environmentally friendly deparaffinization solution (Wuhan Saiwei Biotechnology Co., Ltd., G1128). The sections were hydrated through a graded ethanol series (100%, 95%, and 70%) and distilled water. The hydrated sections were stained with hematoxylin (Wuhan Saiwei Biotechnology Co., Ltd., G1004) for 3 min, rinsed with tap water for 1 min, differentiated with hematoxylin differentiation solution (Wuhan Saiwei Biotechnology Co., Ltd., G11039) for a few seconds, and rinsed with tap water. Hematoxylin blue solution was used to blue the sections, followed by a rinse with running water. The sections were stained with eosin (Wuhan Saiwei Biotechnology Co., Ltd., G1002) and washed with tap water. The slices were dehydrated through a graded ethanol series (75%, 85%, 100%, 5 min each), cleared in *n*-butanol (Sinopharm Chemical Reagent Co., Ltd., 100052190, Shanghai, China) and xylene (Sinopharm Chemical Reagent Co., Ltd., 10023418, Shanghai, China) for 5 min each, and mounted in the mounting medium. The tissues were imaged under a light microscope.

2.14. Immunohistochemical analysis

Mouse colons were fixed with 4% paraformaldehyde, embedded in paraffin, and sectioned into 7 μm slices. The sections were dewaxed using an environmentally friendly dewaxing solution (Wuhan Saiwei Biotechnology Co., Ltd., G1128) and subjected to antigen retrieval using 20 × citric acid antigen retrieval solution (pH 6.0) (Wuhan Saiwei Biotechnology Co., Ltd., G1202), 20 × Tris-EDTA antigen retrieval solution (pH 9.0) (Wuhan Saiwei Biotechnology Co., Ltd., G1203), and 20 × Tris-EDTA antigen retrieval solution (pH 8.0) (Wuhan Saiwei Biotechnology Co., Ltd., G1206). Endogenous peroxidase activity was blocked with 3% H_2O_2. The sections were blocked with 3% BSA and 5% goat serum, incubated overnight with the primary antibody, followed by incubation with a specific secondary antibody and enzyme-labeled streptavidin. DAB chromogenic solution (Wuhan

Saiwei Biotechnology Co., Ltd., G1212) was added dropwise to the sections. The sections were counterstained with hematoxylin (Wuhan Saiwei Biotechnology Co., Ltd., G1004), dehydrated using a graded ethanol series, and mounted. The tissues were imaged under a light microscope.

2.15. Biochemical analyses

Blood samples were harvested from the eyeballs of 25 mice (G1 = PBS; G2 = 2% DSS; G3 = 2% DSS + EcN$\Delta_{pMUT1/2}$; G4 = 2% DSS + EcN-ePDL1-mFc; G5 = 2% DSS + EcN-ePDL1-mFc + Ara (2 g/L)), allowed to stand at room temperature for 1 h, and centrifuged at 2700×*g* (Eppendorf, Centrifuge 5702 R/RH-FastTemp). The supernatant was collected and frozen at −80 °C until analysis. The concentrations of alanine aminotransferase (ALT), aspartate aminotransferase (ASP), alkaline phosphatase (ALP), and urea were measured in the supernatant using a biochemical analyzer within 30 days of sample collection.

Blood samples were collected from the eyeballs of 10 mice (PBS, EcN-ePDL1-mFc + Ara (2 g/L)), left to stand for 1 h at room temperature, and centrifuged at 2700×*g*. Collect the supernatant and freeze at −80 °C until analysis. Within 30 days of sample collection, alanine aminotransferase (ALT), aspartate aminotransferase (ASP), alkaline phosphatase (ALP), total leukocyte count (WBC), hematocrit (HCT), total erythrocyte volume (RBC), mean corpuscular volume (MCV), mean corpuscular hemoglobin content (MCH), mean corpuscular hemoglobin concentration (MCHC), hemoglobin (HGB), Concentration of total platelet count (PLT).

Hierarchical tree and linear discriminant analysis effect size analyses were performed using a cloud platform (Meggie Biomedical Technology Co., Ltd., Shanghai, China).

2.16. Statistical analysis

Immunoblot assays were performed independently three times, and representative blots were displayed. Histological samples were evaluated by two pathologists who were unaware of the treatment details. One image was taken for each histology slide, and a representative image was chosen. Unless specified otherwise, all error bars represent the standard deviation (SD) values. The number of replicates and groups for all *in vitro* experiments is indicated in the figure legends. Flow cytometry data were analyzed using NovoExpress software version 1.5.6. Immunohistochemical data were analyzed using CaseViewer software version 2.4.0.119028 (Biossci, CaseViewer Software Version 2.4.0.11902, Wuhan, China). Statistical analyses were conducted using GraphPad Prism version 8.3.0 (GraphPad Software, Version 8.3.0, San Diego, CA, USA). The significance of differences between means was determined by Student's *t*-test.

3. Results and discussion

3.1. Design and characteristics of recombinant Escherichia coli strain and attachment of ePD-L1-mFc to bacterial outer membrane vesicles

Endogenous cryptic plasmids *pMUT1* and *pMUT2* and recombinant plasmids impose a metabolic burden on EcN and compete for essential transformation resources[39]. Moreover, *pMUT1* and *pMUT2* exacerbate antibiotic resistance, which is a cause for concern given the frequent use of antibiotics for IBD treatment. Consequently, these plasmids may reduce the therapeutic efficacy of EcN therapeutic against IBD[40]. *pMUT1* and *pMUT2* were removed from wild-type EcN using CRISPR/Cas9 technology and a replicon incompatibility strategy to produce EcN$\Delta_{pMUT1/2}$ (Fig. 2A). Electrophoresis results indicated that the knockout strains were stably constructed (Fig. 2B). The analysis of absorbance at 600 nm showed that plasmid excision did not significantly affect bacterial growth (Fig. 2C). Then, a pBAD-mBaoJin expression plasmid carrying the L-arabinose-inducible *E. coli* araBAD promoter and the ara-C regulator was transfected into EcN$\Delta_{pMUT1/2}$[41]. Fluorescence and immunoblot experiments demonstrated that recombinant protein expression was significantly higher in EcN$\Delta_{pMUT1/2}$ than in wild-type EcN (Fig. 2D). Therefore, we choose EcN$\Delta_{pMUT1/2}$ as chassis bacteria, pBAD-ClyA-ePD-L1 and pBAD-ClyA-ePD-L1-mFc were separately inserted into EcN$\Delta_{pMUT1/2}$ to produce the EcN$\Delta_{pMUT1/2}$-ClyA-ePD-L1 strain (EcN-ePD-L) and EcN$\Delta_{pMUT1/2}$-ClyA-mPD-L1-mFc strain (EcN-ePD-L1-mFc) (Fig. 2E). Firstly, we utilized a gradient of arabinose concentrations to induce the expression of the EcN-ePD-L1-mFc strain. Experimental results indicated that a concentration of 2 g/L was optimal for inducing expression, and this was subsequently chosen as the working concentration. Following induction at this level, protein quantification revealed that approximately 2 μg of recombinant protein was produced in 50 mL of bacterial culture (Supporting Information Fig. S1A and S1B). The bacteria were induced with arabinose (2 g/L) for 12 h, and ePD-L1 expression in bacterial lysates was measured by Western blot analysis, the results showed that the presence of the mFc fragment significantly enhanced ePD-L1 expression. The results also showed that ePD-L1 was strongly expressed on OMVs, confirming the successful construction of ePD-L1-mFc and its high expression on OMVs (Fig. 2F). To explore whether the constructed engineered bacteria EcN$\Delta_{pMUT1/2}$ changed the properties of OMVs, we used TEM and DLS to analyze the characteristics of OMVs. The results of TEM and DLS showed that OMVs were double-layered and uniformly spherical, with a diameter of 100−150 nm and zeta potential of −20 mV. There were no significant differences in these parameters between EcN$\Delta_{pMUT1/2}^{OMVs}$ and EcN-ePD-L1-mFc^{OMVs} (Fig. 2G−I).

3.2. Biological activity of recombinant EcN strains in vitro

To assess the biodistribution and pharmacokinetics of EcN$\Delta_{pMUT1/2}$ and EcN-ePD-L1-mFc, these molecules were orally administered to mice and induced with arabinose. Bioluminescence analysis revealed that EcN-ePD-L1-mFc migrated from the gastric mucosa to the gastrointestinal tract 6 h after administration compared to control, with the cecum being the primary site of residence at this time. After 12 h, the colon residence rate of EcN-ePD-L1-mFc was significantly increased, indicating that it was able to tolerate acidic environments and retain in the intestine. After 24 h, the bioluminescence signal weakened because of bacterial clearance, which is crucial for the biosafety of oral biologics (Fig. 3A). The EcN-ePD-L1-mFc variant had a longer residence time in the intestine, likely due to Fc fragment expression, which allowed bacteria to interact with host Fc receptors. This interaction may reduce recognition and elimination by the immune system, providing an "immune camouflage" that enhances bacterial survival. Additionally, the Fc fragment may strengthen adhesion to host cells and help regulate local immune responses, promoting a balanced intestinal microbiome and

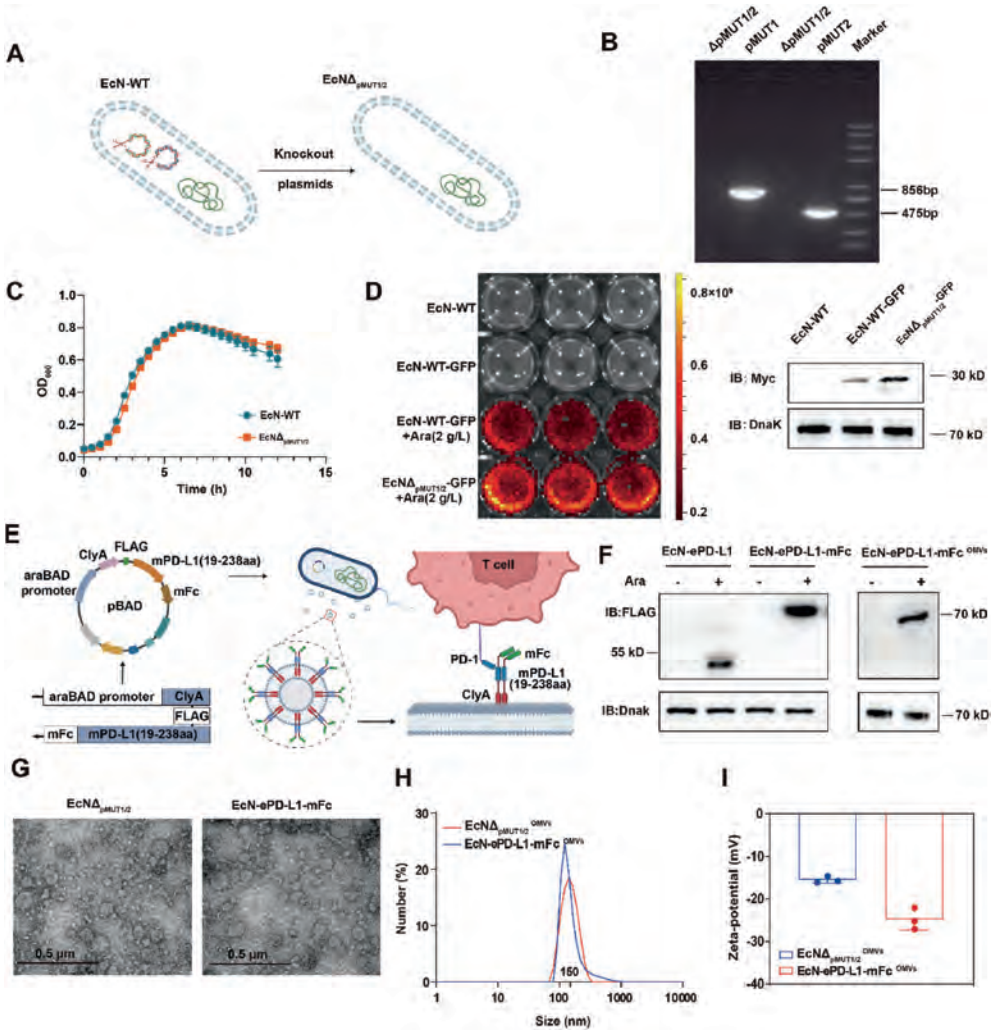

Figure 2 Design and characteristics of recombinant *Escherichia coli* strains and attachment of ePD-L1-mFc to bacterial outer membrane vesicles. (A) Development of the knockout strain EcN$\Delta_{pMUT1/2}$. The endogenous plasmids pMUT1 and pMUT2 in wild-type EcN were knocked out by CRISPR/Case9 technology combined with the replicon in affinity strategy, and the strain EcN$\Delta_{pMUT1/2}$ was constructed. (B) Agarose gel electrophoresis of EcN$\Delta_{pMUT1/2}$ verified successful knockout of endogenous plasmids pMUT1 and pMUT2. The molecular size of the DNA fragment amplified from the pMUT1 is 856 bp, and the molecular size of the DNA fragment amplified from the pMUT2 is 475 bp. (C) Growth profile of wild-type EcN and EcN$\Delta_{pMUT1/2}$ ($n = 5$ per group). (D) Wild-type Nissle 1917 strain and recombinant strain transfected with pBAD-mBaojin plasmid in response to arabinose-induced protein expression. Fluorescence intensity (left), protein expression detected by immunoblot (right). (E) Engineering of the strain EcN-ePD-L1-mFc. The recombinant plasmid ClyA-FLAG-mPDL1(19-238aa)-mFc was transferred into EcN$\Delta_{pMUT1/2}$ after knockout of the endogenous plasmid, and the recombinant strain was denoted as EcN-ePD-L1-mFc. (F) Western blow analysis of recombinant protein expression in EcN-ePD-L1, EcN-ePD-L1-mFc, and outer membrane vesicles (OMVs). (G, H) Transmission electron microscopy analysis of the shape and size distribution of OMVs secreted by recombinant strains. Scale bar = 0.5 μm. (I) Zeta potential of OMVs secreted by recombinant strains, data are mean ± SD of three independent experiments.

supporting probiotic persistence. Enema experiments were conducted to assess the ability of OMVs to penetrate the intestinal epithelial barrier *in vivo*. After anesthetizing mice and ligating the colon, labeled OMVs were injected into the lumen of the ligated colon and incubated at a constant temperature of 37 °C for 2 h. Then, the ligated colon was excised for immunofluorescence analysis. Cell nuclei were stained with DAPI (blue), and EcN-ePD-L1-mFc^{OMVs} were incubated with anti-PD-L1 antibodies (green) (Fig. 3B, Supporting Information Fig. S2A). In addition, we gaved the mouse engineered bacterium EcN-ePDL1-mFc (1×10^9 cfu) and orally administered 2 g/L arabinose to induce protein expression. Intestinal circumcision is performed at 8, 10, and 12 h after gavage to track the course and depth of OMV penetration into the intestinal epithelial barrier. Nuclei were stained with DAPI (blue) and incubated with EcN-ePD-L1-mFc^{OMVs} and anti-PD-L1 antibody (red) (Fig. S2B). The results showed that the OMVs secreted by EcN-ePD-L1-mFc effectively penetrated the epithelial barrier. We also examined the ability of EcN-ePD-L1-mFc to regulate the immune system. OMVs (50 μg) from EcN$\Delta_{pMUT1/2}$ and EcN-ePD-L1-mFc were incubated with DCs in the presence of arabinose to assess the ability of OMVs to bind to DCs *in vitro*. The results showed that EcN-ePD-L1-mFc^{OMVs} bound faster and more extensively to DCs than EcN$\Delta_{pMUT1/2}{}^{OMVs}$ (Fig. S2C).

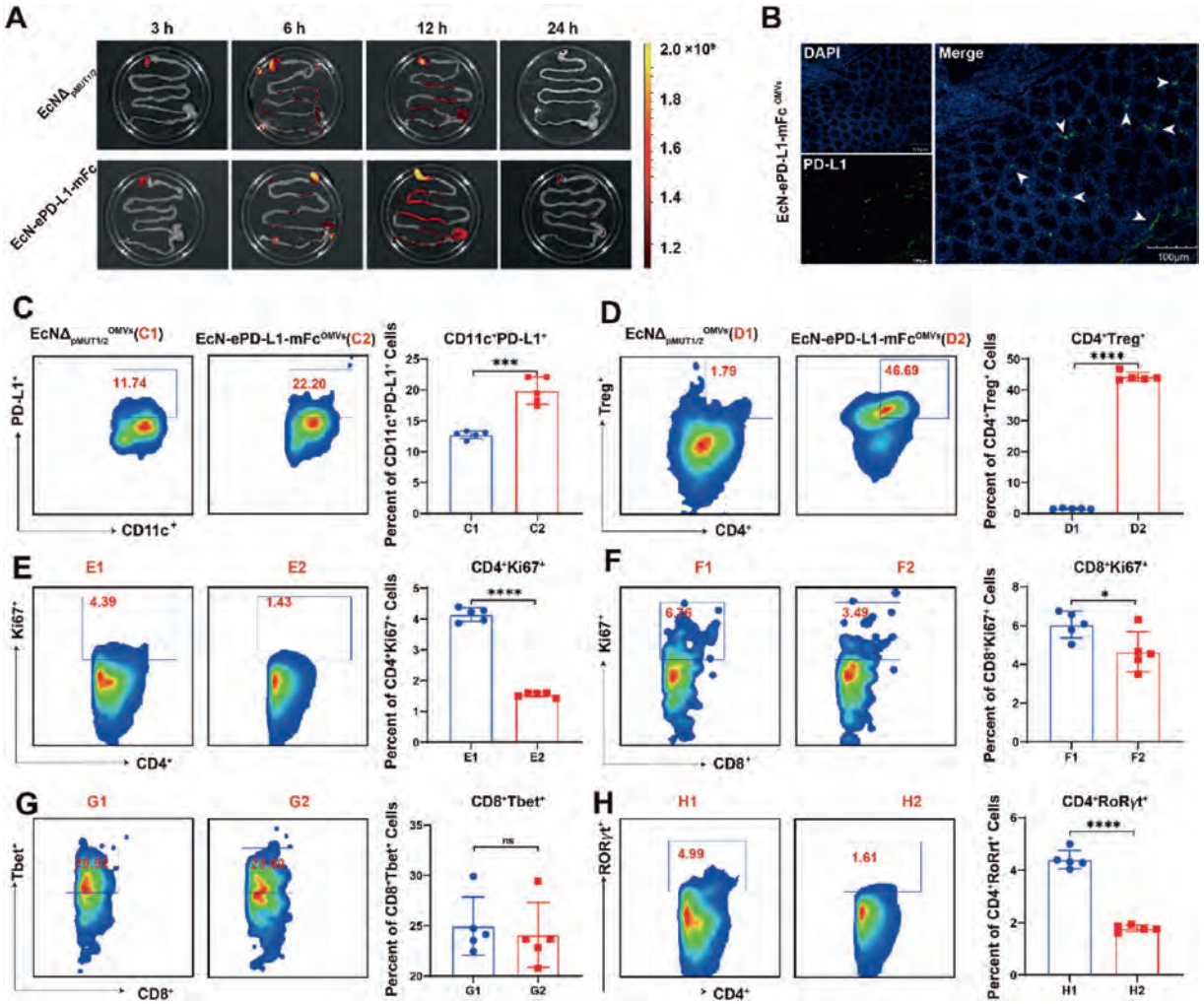

Figure 3 Biological activity of recombinant EcN strains *in vitro*. (A) Fluorescence images of EcNΔ$_{pMUT1/2}$ and EcN-ePD-L1-mFc spatiotemporally resident in the gastrointestinal tract of mice. (B) Immunofluorescence analysis of the penetration of outer membrane vesicles (EcNΔ$_{pMUT1/2}^{OMV}$(50 μg) and EcN-ePDL1-mFc ^{OMVs}) secreted by recombinant strains in the epithelia of ligated intestines of fasted mice. (C−H) Flow cytometry analysis of the effect of EcNΔ$_{pMUT1/2}^{OMV}$(50 μg) and EcN-ePDL1-mFc ^{OMVs} on the number of mouse spleen immune cells ($n = 5$). Data (C−H) are presented as the mean ± SD of five independent experiments. *P* values were calculated by *t*-test. $^{*}P < 0.05$, $^{***}P < 0.001$, $^{****}P < 0.0001$; ns, no significance.

Given that IBD is characterized by immune cell infiltration in the colon, we assessed the effects of EcN-ePD-L1-mFc on immune cells. The spleens of C57BL/6 mice were removed and homogenized, and cell suspensions were incubated with OMVs from EcNΔ$_{pMUT1/2}$ and EcN-ePD-L1-mFc. Flow cytometry results showed that the proportion of CD11c^{+} PD-L1^{+} cells was significantly higher in EcN-ePD-L1-mFc^{OMVs} than in EcNΔ$_{pMUT1/2}^{OMVs}$, demonstrating strong binding and enrichment of ePD-L1-mFc to DCs (Fig. 3C). The percentage of CD4^{+} Treg cells was significantly higher, whereas the percentage of CD4^{+} Ki67^{+} and CD8^{+} Ki67^{+} T cells was markedly lower in EcN-ePD-L1-mFc^{OMVs}, indicating a significant decrease in T cell proliferation in this group (Fig. 3D−F). Similarly, the percentage of CD8^{+} T-bet^{+} T cells and CD4^{+} RORγt $^{+}$ T cells was significantly lower in EcN-ePD-L1-mFc^{OMVs}. T-bet regulates effector CD8^{+} T cell function, and RORγt may be implicated in Th17 differentiation[42,43] (Fig. 3G and H; Fig. S2D). These results suggest that when the ePD-L1 protein on OMVs binds to the PD-1 receptor on effector T cells, it activates an inhibitory signaling pathway within the T cells, leading to the downregulation of T cell receptor (TCR) signaling and subsequent inhibition of effector T cell proliferation[44]. In addition to transmitting inhibitory signals to T cells, this interaction can also induce the differentiation of effector T cells into induced T regulatory cells (iTregs), promoting their proliferation and maintaining their function[45]. Therefore, in the OMVs group of engineered bacteria used in this study, we propose that this effect is mediated by the PD-L1-Fc protein, which not only directly inhibits effector T cell proliferation but also further promotes immune regulation and balance in IBD lesions through the immunosuppressive effects of Tregs.

3.3. ePD-L1-mFc-expressing EcN improves dextran sulfate sodium-induced ulcerative colitis in mice

To assess the therapeutic efficacy of EcN-ePD-L1-mFc in a mouse model of DSS-induced IBD, mice were assigned to different treatments: PBS (group 1), 2% DSS (groups 2), DSS + EcNΔ$_{pMUT1/2}$ (group 3), DSS + EcN-ePD-L1-mFc (group

4), and DSS + EcN-ePD-L1-mFc + arabinose (group 5). Group 5 was treated with arabinose (2 g/L) for 12 h after administering DSS + EcN-ePD-L1-mFc to induce the protein expression of ePD-L1-mFc (Fig. 4A; Supporting Information Fig. S3A). The results showed that DSS tended to decrease body weight in groups G2, G3, and G4, whereas arabinose-induced EcN-ePD-L1-mFc expression in G5 mitigated this effect. Additionally, no statistically significant difference in colon length was observed between groups 2 and 4, whereas a significant difference was noted between groups 2 and 5, as well as between groups 4 and 5, suggesting that EcN-ePD-L1-mFc, when induced by arabinose, effectively alleviates inflammatory bowel disease (Fig. 4B). Considering that colon length indicates disease severity and treatment effectiveness in animal models, we measured changes in

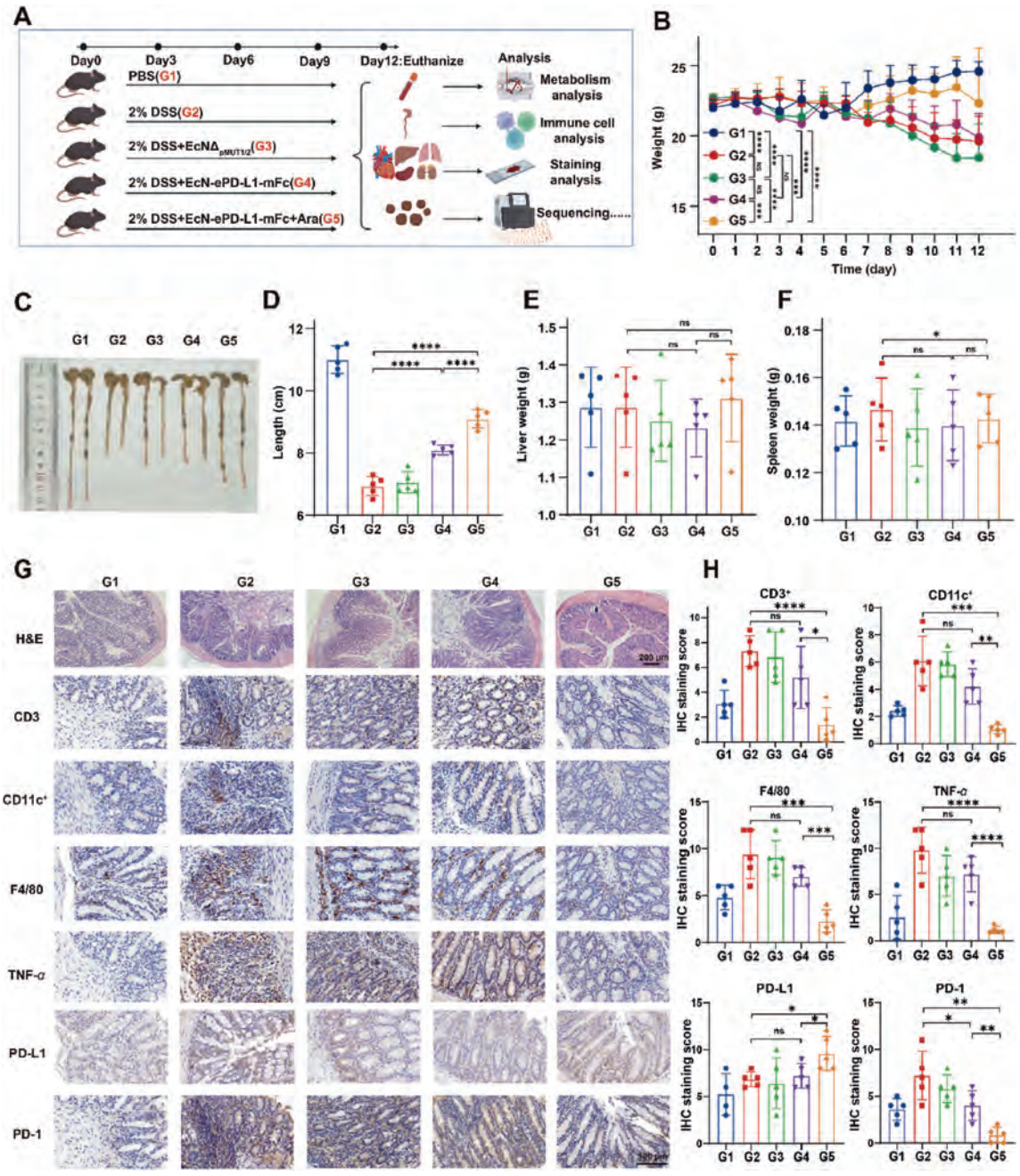

Figure 4 ePD-L1-mFc-expressing EcN improves dextran sulfate sodium-induced ulcerative colitis in mice. (A) Schematic diagram of the treatment of experimental and control animals. PBS, 2% DSS, 2% DSS + EcN$\Delta_{pMUT1/2}$, 2% DSS + EcN-ePDL1-mFc, 2% DSS + EcN-ePDL1-mFc, 2% DSS + EcN-ePDL1-mFc + Ara (2 g/L) was administered at a concentration of 1.0×10^9 CFU on Days 0, 3, 6 and 9 ($n = 5$). (B) Body weight of each group. (C, D) Colonic length in each group on Day 12. (E, F) Liver and spleen weight in different groups on Day 12. (G) Histological analysis of mouse colonic tissue (hematoxylin−eosin). Scale bar = 100 μm. (H) Immunohistochemical expression of CD3, CD11c$^+$, F4/80, TNF-α, PD-1, and PD-L1 in mouse colonic tissue (five animals per group). All data are presented as the mean ± SD of independent experiments. P values were calculated by t-test.*$P < 0.05$, **$P < 0.01$, ***$P < 0.001$, ****$P < 0.0001$; ns, no significance.

colon length in mice and found that EcN-ePD-L1-mFc reduced the effect of DSS (Fig. 4C and D; Fig. S3B), indicating that ePD-L1-mFc-expressing EcN alleviates IBD symptoms. In contrast, there were no significant between-group differences in liver and spleen weight (Fig. 4E and F).

H&E and immunohistochemical staining revealed that the levels of the T cell marker $CD3^+$, DC marker $CD11c^+$, macrophage marker F4/80, monocyte-macrophage-secreted pro-inflammatory cytokine TNF-α, and PD-1 were significantly lower in ePD-L1-mFc-expressing EcN than in the other groups, while PD-L1 expression was significantly higher in the arabinose-induced group (Fig. 4G and H). These results indicate that the ePD-L1-mFc-expressing strain reduces IBD by inhibiting the infiltration of inflammatory cells, including T cells, DCs, and macrophages.

3.4. The mechanism by which EcN-ePD-L1-mFc reduces inflammatory bowel disease

The immunomodulatory effect of EcN-ePD-L1-mFc was assessed in mice with acute IBD by flow cytometric analysis of $CD4^+$ and $CD8^+$ T cell populations in mesenteric lymph nodes. The results showed that DSS tended to increase the number of $CD4^+$ $CD69^+$ T cells, while ePD-L1-mFc expression tended to reduce this effect, suggesting that ePD-L1-mFc expression inhibited the activation of $CD4^+$ T cells. Similar results were obtained in $CD4^+$ $IL17^+$ T cells. In contrast, DSS tended to decrease the number of natural regulatory T cells ($CD4^+$ $Foxp3^+$), and ePD-L1-mFc expression mitigated this effect (Fig. 5A and B). The impact of ePD-L1-mFc on other immune cell subpopulations was not significant (Supporting Information Fig. S4A).

Flow cytometry analysis showed no significant differences in the number of $CD4^+$ and $CD8^+$ T cell populations in the spleen, suggesting that the primary anti-inflammatory activity, particularly inhibition of IL-17 secretion, is mediated by the intestinal immune system (Fig. S4B and S4C). Given that IBD is characterized by intestinal mucosal barrier injury, the expression of intestinal mucosal barrier markers claudin-1 and occludin was evaluated by immunohistochemistry. Claudin-1 and occludin expression were significantly higher in the ePD-L1-mFc-expressing group than in the DSS group, suggesting that ePD-L1-mFc expression improves intestinal barrier integrity and function (Fig. 5C and D). Additionally, TUNEL staining showed that DSS increased intestinal apoptosis, and ePD-L1-mFc expression reversed this effect (Fig. 5E and F). These results demonstrate that ePD-L1-mFc-expressing EcN inhibits IBD by reducing IL-17 expression, improving intestinal barrier function, and inhibiting apoptosis.

3.5. ePD-L1-mFc-expressing EcN alleviates dextran sulfate sodium-induced dysbiosis in the mouse intestine

The pathogenesis of IBD involves alterations in gut microbiota, including the reduced diversity and abundance of SCFA producers and the increased abundance of pro-inflammatory microorganisms, including adhesive and invasive *E. coli* strains and hydrogen sulfide producers[46,47]. We studied the effect of ePD-L1-mFc-expressing EcN on intestinal microbial composition by bacterial 16S rRNA sequencing of intestinal contents. High-quality sequences with $\geq$97% similarity were clustered into operational taxonomic units (OTUs). The results indicated that the ePD-L1-mFc-expressing strain significantly increased bacterial diversity and abundance in the mouse intestine (Fig. 6A, Supporting Information Fig. S5A). Overall differences in fecal bacterial communities were analyzed by principal coordinate analysis. The findings showed that bacterial communities in animals treated with ePD-L1-mFc-expressing EcN were closer to those of the PBS group, while the communities in the other three groups clustered together, indicating that EcN-ePD-L1-mFc reshaped the intestinal microbiota (Fig. 6B). Venn diagrams revealed that 317 OTUs were shared across the five groups, and G1, G2, and G5 had 99, 39, and 46 unique OTUs. G1 and G2 shared 60 unique OTUs, G1 and G5 shared 127, and G2 and G5 shared 75, suggesting that the PBS group was more similar to the group inoculated with ePD-L1-mFc-expressing EcN and less similar to the DSS-treated groups (Fig. S5B). The analysis at the genus level showed that DSS increased the relative abundance of *Bacteroides*, whereas ePD-L1-mFc-expressing EcN reversed this effect and increased the abundance of *norank_f__Muribaculaceae* and *Lachnospiraceae_NK4A136*_group, indicating that treatment with ePD-L1-mFc-expressing EcN restored the intestinal microbiota at the genus level and increased the abundance of *norank_f__Muribaculaceae* and *Lachnospiraceae_NK4A136*_group, which improve digestive and immune function by maintaining gut microbiota balance (Fig. 6C). Univariate analysis of the 10 most abundant genera showed that DSS increased the relative abundance of *Bacteroides*, *Helicobacter*, and *Parabacteroides*, while ePD-L1-mFc-expressing EcN restored the levels of *Lachnospiraceae_NK4A136*_group and *norank_f__norank_o__Clostridia_UCG-014*, indicating that the engineered strain changed the abundance of members of the Lachnospiraceae family (Fig. S5C). Heatmap analysis showed that the DSS group increased the relative abundance of *Bacteroides* while ePD-L1-mFc-expressing EcN increased the abundance of *norank_f__Muribaculaceae* and *Lachnospiraceae_NK4A136*_group (Fig. 6D, Fig. S5D). Hierarchical tree and linear discriminant analysis effect size analysis of differentially enriched taxa yielded similar results. Moreover, bacterial abundance and richness were significantly higher in the group inoculated with ePD-L1-mFc-expressing EcN than in DSS-treated mice (Fig. 6E and F). The function of the gut microbiota was predicted by combining PICRUSt2 with the MetaCyc database. There were differences in amino acid metabolism, carbohydrate biosynthesis and metabolism, and fatty acid metabolism among the groups. EcN-PD-L1-mFc-expressing EcN promoted the carbohydrate biosynthesis and metabolism and amino acid metabolism of intestinal microorganisms (Fig. S5E). These metabolic alterations may influence host immune responses by modulating the production of microbial metabolites.

SCFAs are an important energy source for intestinal epithelial cells and enhance intestinal barrier function[48,49]. Active IBD is characterized by decreased levels of SCFAs in the stool. The analysis of SCFA concentrations indicated that DSS remarkably reduced the concentrations of acetic, propanoic, butanoic, isobutyric, valeric, and isovaleric acid, whereas ePD-L1-mFc-expressing EcN attenuated this effect (Fig. 6G). These results suggest that ePD-L1-mFc-expressing EcN improves IBD by increasing the abundance of Lachnospiraceae, reducing the abundance of *Bacteroides*, and increasing intestinal SCFA levels.

3.6. In vivo safety of EcN-ePD-L1-mFc

To verify whether orally administered EcN-ePD-L1-mFc affects other organs, we performed H&E staining of sections of the heart, liver, spleen, lungs, and kidneys. There were no between-group differences in histology (Fig. 7A). Biochemical analyses revealed that DSS decreased the serum concentrations of ALP, whereas

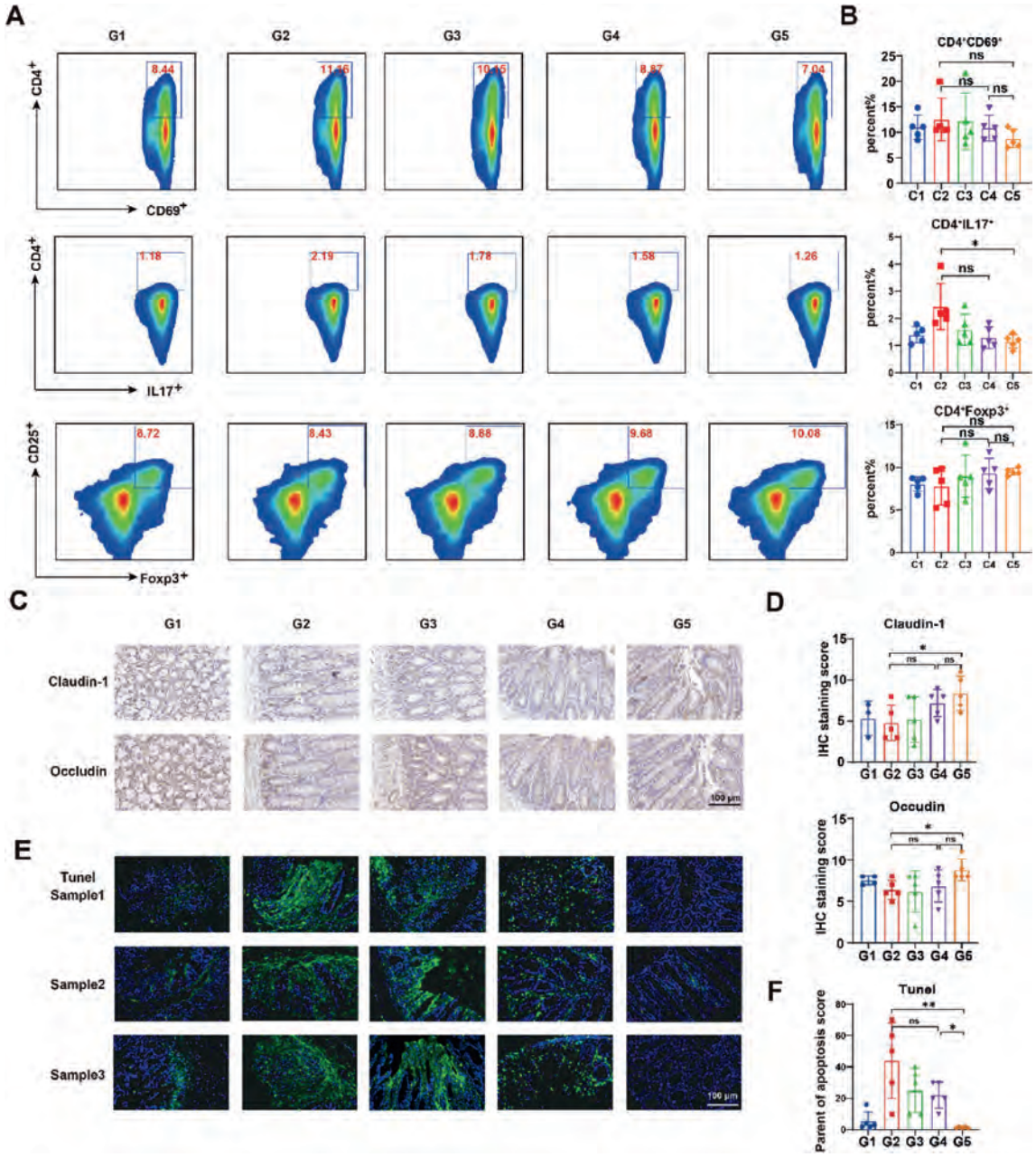

Figure 5 The mechanism by which EcN-ePD-L1-mFc inhibits inflammatory bowel disease in mice. (A, B) Flow cytometry analysis of the expression of $CD69^+$, $IL17^+$, and $CD4^+Foxp3^+$ T cells in mesenteric lymph nodes across groups (G1 = PBS; G2 = 2% DSS; G3 = 2% DSS + EcNΔpMUT1/2; G4 = 2% DSS + EcN-ePDL1-mFc; G5 = 2% DSS + EcN-ePDL1-mFc + Ara (2 g/L)) (n = 5). (C, D) Immunohistochemical expression of claudin-1 and occludin in colon tissue. Scale bar = 100 μm (n = 5). (E, F) TUNEL staining of colon tissue. Scale bar = 100 μm (n = 5). All Data are presented as the mean ± SD of independent experiments. P values were calculated by t-test. $^*P < 0.05$, $^{**}P < 0.01$; ns, no significance.

ePD-L1-mFc-expressing EcN reversed this effect. In contrast, the interventions did not significantly affect the serum concentrations of alanine aminotransferase (ALT), aspartate aminotransferase (AST), and urea (Fig. 7B). In addition, the engineered bacteria were evaluated for safety for 30 Days. Mice (n = 5) were given PBS or EcN-ePD-L1-mFc (1×10^9 cfu) plus Ara (2 g/L) orally every 3 days. Monitoring of mouse body weights revealed no statistically significant differences between the two groups. On Day 30, blood was collected by ocular puncture for complete blood count (CBC) and liver and kidney function analysis. The results showed that all blood counts were within the normal range, as were markers of liver and kidney function (*e.g.*, ALT, AST) (Supporting Information Fig. S6A and S6B). These results indicate that enteritis is associated with increased ALP levels and that the engineered EcN-ePD-L1-mFc does not affect other organs and are thus a promising candidate for the local treatment of IBD.

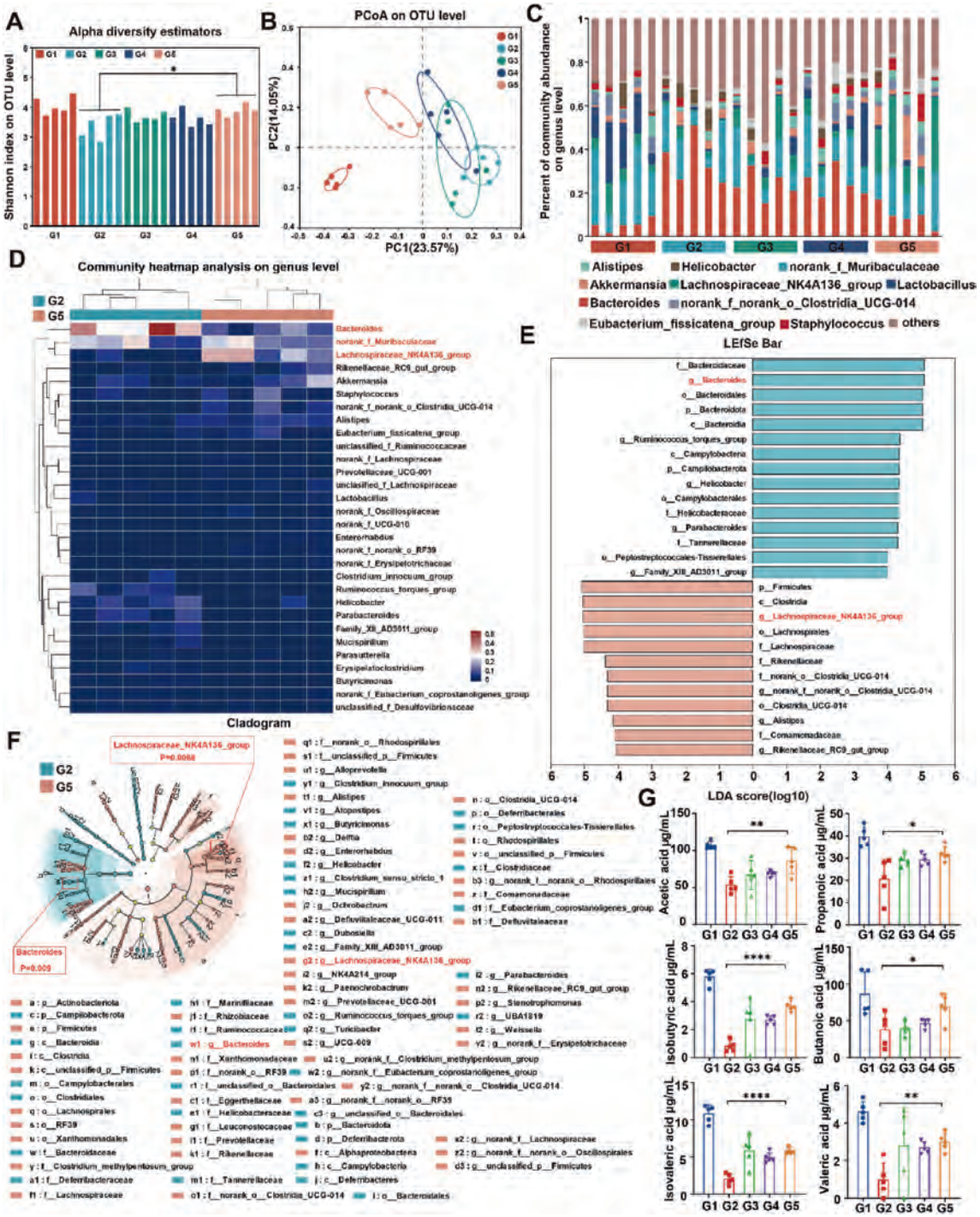

Figure 6 ePD-L1-mFc-expressing EcN alleviates dextran sulfate sodium-induced dysbiosis in the mouse intestine. (A, B) Alpha diversity (Shannon indexes) and beta diversity (principal coordinate analysis) in the mouse intestine in each treatment group (G1 = PBS; G2 = 2% DSS; G3 = 2% DSS + EcNΔpMUT1/2; G4 = 2% DSS + EcN-ePDL1-mFc; G5 = 2% DSS + EcN-ePDL1-mFc + Ara (2 g/L), $n = 5$). (C) Bacterial abundance at the genus level in the intestine. (D) Most representative bacterial taxa in the intestine of mice treated with 2% DSS (group 2) or EcN-ePD-L1-mFc (group 5). (E) Linear discriminant analysis (LDA) effect size analysis of differentially enriched bacterial taxa in the intestine of groups 2 and 5; LDA>4. (F) Hierarchical tree of differentially enriched bacterial taxa in the gut of groups 2 and 5; LDA>3. (G) Concentrations of short-chain fatty acids in the mouse cecum. Data are means ± SD of independent experiments. *P* values were calculated by *t*-test. $^{*}P < 0.05$, $^{**}P < 0.01$, $^{****}P < 0.0001$.

4. Discussion and conclusions

IBD is a complex autoimmune disease characterized by immune dysregulation, excessive activation of Th cells, and production of pro-inflammatory mediators in the gut. Immunosuppressive medications may cause severe side effects, making probiotics particularly important. However, the therapeutic efficacy and intestinal retention of probiotics are limited. We addressed this limitation by

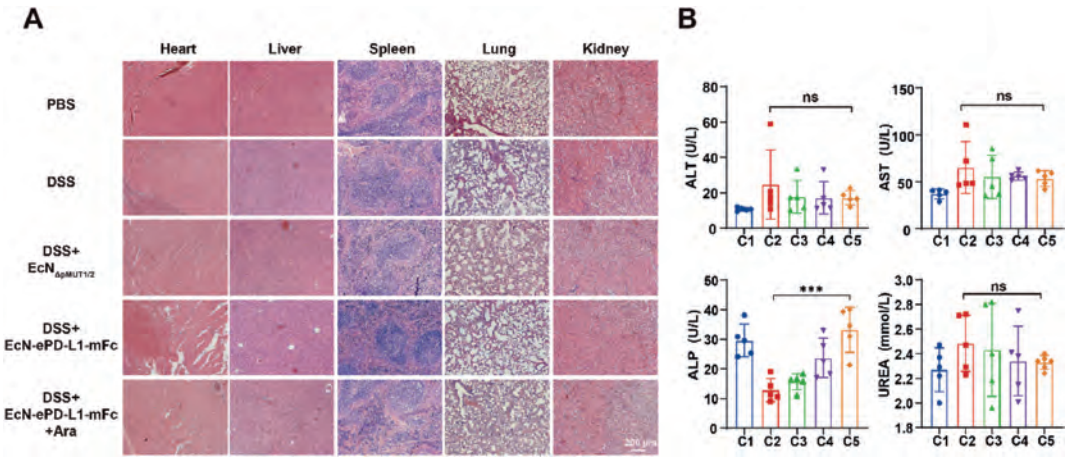

Figure 7 Effect of EcN-ePD-L1-mFc on different organs. (A) Representative images of the heart, liver, spleen, lung, and kidney of mice in each group. (B) Serum concentrations of alanine aminotransferase (ALT), aspartate aminotransferase (AST), alkaline phosphatase (ALP), and urea in different groups ($n = 5$). All Data are presented as the mean ± SD of independent experiments. P values were calculated by t-test. $^{***}P < 0.001$; ns, no significance.

engineering the probiotic EcN. First, we removed the endogenous plasmids pMUT1 and pMUT2 to enhance recombinant protein expression. Then, we attached the PD-L1-mFc fusion protein to the bacterial surface using a ClyA fragment to enhance the stable expression of PD-L1 (19−238 aa) and its presentation on OMVs. This approach allowed the stable construction of EcN-ePD-L1-mFc. Immunological assays showed that EcN-ePD-L1-mFc^{OMVs} effectively inhibited immune cell function and proliferation. Further, EcN-ePD-L1-mFc^{OMVs} alleviated IBD in mice by decreasing the percentage of T cells, DCs, and macrophages, downregulating inflammatory cytokines, improving intestinal barrier function, and inhibiting apoptosis. The analysis of intestinal contents and metabolites showed that the engineered bacteria had beneficial effects by increasing the abundance of Lactobacillaceae, decreasing the abundance of *Bacteroides*, and increasing the intestinal concentrations of SCFAs. This study highlights three primary benefits of the engineered probiotic strategy: firstly, targeted drug delivery for intestinal diseases, minimizing systemic side effects; secondly, simultaneous regulation of the intestinal immune response and microbial environment by probiotics; and thirdly, the cost-effectiveness and high patient compliance of this treatment approach. This strategy offers a promising avenue for future intestinal disease therapies.

In recent years, many studies have focused on using engineered bacteria to deliver protein therapeutics or improve gut microbiota for treating IBD[50,51]. In clinical practice, the engineered bacterium EcN-ePD-L1-mFc, constructed using the probiotic *E. coli* Nissle 1917, could potentially change the treatment paradigm for IBD, as it provides a therapeutic option that directly interacts with immune cells at the site of inflammation, offering a more targeted and personalized approach. For example, by promoting Treg proliferation and inhibiting effector T cell activation, this strategy could help restore immune tolerance within the gut and potentially reduce the need for long-term immunosuppressive therapies. Additionally, the ability of EcN-ePD-L1-mFc to enhance intestinal epithelial barrier repair and restore microbiota balance makes it a promising therapeutic agent that addresses not only inflammation but also the dysbiosis commonly seen in IBD patients. However, clinical translation requires careful consideration of several factors. First, while engineered bacteria show significant efficacy in preclinical models, their safety and efficacy in human subjects must be rigorously tested through clinical trials. The immunomodulatory potential of ePD-L1-mFc needs to be further validated to ensure it does not inadvertently impair normal immune responses or cause immune-related adverse events. Furthermore, the production, formulation, and long-term stability of engineered EcN strains for clinical use must be optimized, with attention to regulatory and ethical considerations surrounding the use of genetically modified organisms (GMOs). The therapeutic potential of EcN-ePD-L1-mFc in IBD represents a promising example of precision medicine, where gut-targeted therapies could offer a safer and more effective alternative to conventional immunosuppressive treatments. Moving forward, we believe that clinical trials will be essential to fully assess the safety, dosing regimen, and therapeutic efficacy of this innovative approach for IBD patients.

SCFAs, as key energy sources for intestinal epithelial cells, play a crucial role in enhancing intestinal barrier function and maintaining immune homeostasis in the gut[52]. Active IBD is characterized by reduced levels of SCFAs in the stool. In our experiments, DSS treatment significantly reduced the concentrations of acetic acid, propionic acid, butyric acid, isobutyric acid, valeric acid, and isovaleric acid, whereas the EcN-PD-L1-mFc-expressing strain attenuated this effect. These results suggest that EcN-PD-L1-mFc improves IBD by increasing SCFA levels. SCFAs have an essential role in immune regulation. They not only provide energy to intestinal epithelial cells but also influence local immune responses through various mechanisms[53]. SCFAs mediate anti-inflammatory effects by activating G-protein-coupled receptors (such as GPR41 and GPR43), which modulate T cell functions, particularly promoting the differentiation of regulatory T cells (Tregs) and thus suppressing excessive immune activation and inflammation. Additionally, SCFAs enhance intestinal barrier function by reducing intestinal permeability, preventing bacterial and endotoxin translocation, and minimizing immune system overactivation. Furthermore, our data showed that EcN-PD-L1-mFc increased the abundance of Lachnospiraceae while decreasing the abundance of *Bacteroides*. Lachnospiraceae are known to be beneficial to gut health, producing abundant SCFAs, whereas an increase in *Bacteroides* has been linked to the

progression of IBD. Thus, EcN-PD-L1-mFc may modulate immune responses through changes in gut microbiota composition and SCFA production, providing a potential therapeutic strategy for IBD.

Acknowledgments

This work was supported by the National Natural Science Foundation of China (Nos. 32371461 and 81873449), Suzhou Health Youth Backbone Talent "National Tutorial System" Training Project (No. Qngg2023005, China), Jiangsu Natural Science Foundation (No. BK20210086, China), Basic Science (Natural Science) Research Program for Universities in Jiangsu Province (No. 24KJB310015, China). Gusu Leading Talent Program for Innovation and Entrepreneurship (No. ZXL2021441, China), the Science and Technology Plan Project of Suzhou (No. SKY2022150, China), Suzhou Science and Technology Bureau Basic Research (No. SSD2024073, China) and Beijing Xisike Clinical Oncology Research Foundation (No. Y-tongshu2021/qn-0366, China). We also thank TopEdit for professional language editing.

Author contributions

Xiaopeng Tian, Kai Yang, Lin Hu and Muxing Zhang conceived and designed the experiments. Yuhong Wang, Lin Hu, Lei Wang, and Xiaopeng Tian wrote and revised the manuscript. Yuhong Wang, Lin Hu, Lei Wang, Chonghai Zhang, Wenhao Shen, Xin Zhang, and Hongli Yang developed the methods. Yuhong Wang, Lin Hu, Mengmeng Xu and Lei Wang analyzed and interpreted the data; Xiaopeng Tian, Kai Yang, Min Li and Muxing Zhang supervised the study. All authors read and approved the final manuscript.

Conflicts of interest

The authors have no conflicts of interest to declare.

Appendix A. Supporting information

Supporting information to this article can be found online at https://doi.org/10.1016/j.apsb.2025.08.002.

References

1. Richard ML, Sokol H. The gut mycobiota: insights into analysis, environmental interactions and role in gastrointestinal diseases. *Nat Rev Gastroenterol Hepatol* 2019;**16**:331−45.
2. Khaloian S, Rath E, Hammoudi N, Gleisinger E, Blutke A, Giesbertz P, et al. Mitochondrial impairment drives intestinal stem cell transition into dysfunctional paneth cells predicting Crohn's disease recurrence. *Gut* 2020;**69**:1939−51.
3. Wu Z, Liu D, Deng F. The role of vitamin D in immune system and inflammatory bowel disease. *J Inflamm Res* 2022;**15**:3167−85.
4. Jeong DY, Kim S, Son MJ, Son CY, Kim JY, Kronbichler A, et al. Induction and maintenance treatment of inflammatory bowel disease: a comprehensive review. *Autoimmun Rev* 2019;**18**:439−54.
5. Dudek P, Fabisiak A, Zatorski H, Malecka-Wojciesko E, Talar-Wojnarowska R. Efficacy, safety and future perspectives of JAK inhibitors in the IBD treatment. *J Clin Med* 2021;**10**:5660.
6. Sayoc-Becerra A, Krishnan M, Fan S, Jimenez J, Hernandez R, Gibson K, et al. The JAK-inhibitor tofacitinib rescues human intestinal epithelial cells and colonoids from cytokine-induced barrier dysfunction. *Inflamm Bowel Dis* 2020;**26**:407−22.
7. Sandborn WJ, Feagan BG, Loftus Jr EV, Peyrin-Biroulet L, Van Assche G, D'Haens G, et al. Efficacy and safety of upadacitinib in a randomized trial of patients with Crohn's disease. *Gastroenterology* 2020;**158**:2123−38.e8.
8. Radeke HH, Stein J, Van Assche G, Rogler G, Lakatos PL, Muellershausen F, et al. A multicentre, double-blind, placebo-controlled, parallel-group study to evaluate the efficacy, safety, and tolerability of the S1P receptor agonist KRP203 in patients with moderately active refractory ulcerative colitis. *Inflamm Intest Dis* 2020;**5**:180−90.
9. Sedda S, Franze E, Bevivino G, Di Giovangiulio M, Rizzo A, Colantoni A, et al. Reciprocal regulation between Smad7 and Sirt1 in the gut. *Front Immunol* 2018;**9**:1854.
10. Garo LP, Ajay AK, Fujiwara M, Beynon V, Kuhn C, Gabriely G, et al. Smad7 controls immunoregulatory PDL2/1-PD1 signaling in intestinal inflammation and autoimmunity. *Cell Rep* 2019;**28**:3353−66.e5.
11. Ma R, Song N, Wang L, Gu X, Xiong F, Zhang S, et al. Discovery of 2-(methylcarbonylamino) thiazole as PDE4 inhibitors *via* virtual screening and biological evaluation. *J Mol Graph Model* 2023;**124**:108567.
12. Spadaccini M, D'Alessio S, Peyrin-Biroulet L, Danese S. PDE4 inhibition and inflammatory bowel disease: a novel therapeutic avenue. *Int J Mol Sci* 2017;**18**:1276.
13. Moschen AR, Tilg H, Raine T. IL-12, IL-23 and IL-17 in IBD: immunobiology and therapeutic targeting. *Nat Rev Gastroenterol Hepatol* 2019;**16**:185−96.
14. Vuyyuru SK, Shackelton LM, Hanzel J, Ma C, Jairath V, Feagan BG. Targeting IL-23 for IBD: rationale and progress to date. *Drugs* 2023;**83**:873−91.
15. de Lange KM, Moutsianas L, Lee JC, Lamb CA, Luo Y, Kennedy NA, et al. Genome-wide association study implicates immune activation of multiple integrin genes in inflammatory bowel disease. *Nat Genet* 2017;**49**:256−61.
16. Bischoff SC, Bager P, Escher J, Forbes A, Hebuterne X, Hvas CL, et al. ESPEN guideline on clinical nutrition in inflammatory bowel disease. *Clin Nutr* 2023;**42**:352−79.
17. Zhang T, Zhang J, Duan L. The role of genetically engineered probiotics for treatment of inflammatory bowel disease: a systematic review. *Nutrients* 2023;**15**:1566.
18. Effendi SSW, Ng IS. Prospective and challenges of live bacterial therapeutics from a superhero Escherichia coli Nissle 1917. *Crit Rev Microbiol* 2023;**49**:611−27.
19. Suez J, Zmora N, Segal E, Elinav E. The pros, cons, and many unknowns of probiotics. *Nat Med* 2019;**25**:716−29.
20. Praveschotinunt P, Duraj-Thatte AM, Gelfat I, Bahl F, Chou DB, Joshi NS. Engineered *E. coli* Nissle 1917 for the delivery of matrix-tethered therapeutic domains to the gut. *Nat Commun* 2019;**10**:5580.
21. Chen RY, Zhu Y, Shen YY, Xu QY, Tang HY, Cui NX, et al. The role of PD-1 signaling in health and immune-related diseases. *Front Immunol* 2023;**14**:1163633.
22. Pauken KE, Torchia JA, Chaudhri A, Sharpe AH, Freeman GJ. Emerging concepts in PD-1 checkpoint biology. *Semin Immunol* 2021;**52**:101480.
23. Jubel JM, Barbati ZR, Burger C, Wirtz DC, Schildberg FA. The role of PD-1 in acute and chronic infection. *Front Immunol* 2020;**11**:487.
24. Roosenboom B, Horjus Talabur Horje CS, Smids C, Leeuwis JW, van Koolwijk E, Groenen MJM, et al. Distribution of mucosal PD-1 expressing T cells in patients with colitis of different etiologies. *Scand J Gastroenterol* 2021;**56**:671−9.
25. Kim MK, Jo SI, Kim SY, Lim H, Kang HS, Moon SH, et al. PD-1-positive cells contribute to the diagnosis of inflammatory bowel disease and can aid in predicting response to vedolizumab. *Sci Rep* 2023;**13**:21329.
26. Chulkina M, Beswick EJ, Pinchuk IV. Role of PD-L1 in gut mucosa tolerance and chronic inflammation. *Int J Mol Sci* 2020;**21**:9165.

27. Rajabian Z, Kalani F, Taghiloo S, Tehrani M, Rafiei A, Hosseini-Khah Z, et al. Over-expression of immunosuppressive molecules, PD-L1 and PD-L2, in ulcerative colitis patients. *Iran J Immunol* 2019;**16**: 62−70.
28. Luoma AM, Suo S, Williams HL, Sharova T, Sullivan K, Manos M, et al. Molecular pathways of colon inflammation induced by cancer immunotherapy. *Cell* 2020;**182**:655−71.e22.
29. Song MY, Hong CP, Park SJ, Kim JH, Yang BG, Park Y, et al. Protective effects of Fc-fused PD-L1 on two different animal models of colitis. *Gut* 2015;**64**:260−71.
30. Xu F, Fei Z, Dai H, Xu J, Fan Q, Shen S, et al. Mesenchymal stem cell-derived extracellular vesicles with high PD-L1 expression for autoimmune diseases treatment. *Adv Mater* 2022;**34**:e2106265.
31. Nielsen DL, Juhl CB, Chen IM, Kellermann L, Nielsen OH. Immune checkpoint inhibitor-induced diarrhea and colitis: incidence and management. a systematic review and meta-analysis. *Cancer Treat Rev* 2022;**109**:102440.
32. Lieberman LA. Outer membrane vesicles: a bacterial-derived vaccination system. *Front Microbiol* 2022;**13**:1029146.
33. Li M, Li S, Zhou H, Tang X, Wu Y, Jiang W, et al. Chemotaxis-driven delivery of nano-pathogenoids for complete eradication of tumors post-phototherapy. *Nat Commun* 2020;**11**:1126.
34. Petousis-Harris H, Paynter J, Morgan J, Saxton P, McArdle B, Goodyear-Smith F, et al. Effectiveness of a group B outer membrane vesicle meningococcal vaccine against gonorrhoea in New Zealand: a retrospective case-control study. *Lancet* 2017;**390**:1603−10.
35. Li Y, Zhao R, Cheng K, Zhang K, Wang Y, Zhang Y, et al. Bacterial outer membrane vesicles presenting programmed death 1 for improved cancer immunotherapy *via* immune activation and checkpoint inhibition. *ACS Nano* 2020;**14**:16698−711.
36. Rappazzo CG, Watkins HC, Guarino CM, Chau A, Lopez JL, DeLisa MP, et al. Recombinant M2e outer membrane vesicle vaccines protect against lethal influenza A challenge in BALB/c mice. *Vaccine* 2016;**34**:1252−8.
37. Pritsch M, Ben-Khaled N, Chaloupka M, Kobold S, Berens-Riha N, Peter A, et al. Comparison of intranasal outer membrane vesicles with cholera toxin and injected MF59C.1 as adjuvants for malaria transmission blocking antigens AnAPN1 and Pfs48/45. *J Immunol Res* 2016;**2016**:3576028.
38. Jiang Y, Chen B, Duan C, Sun B, Yang J, Yang S. Multigene editing in the *Escherichia coli* genome *via* the CRISPR-Cas9 system. *Appl Environ Microbiol* 2015;**81**:2506−14.
39. Zhou S, Zhao L, Zuo W, Zheng Y, Zhang P, Sun Y, et al. Minimizing endogenous cryptic plasmids to construct antibiotic-free expression systems for *Escherichia coli* Nissle 1917. *Synth Syst Biotechnol* 2024; **9**:165−75.
40. Zainuddin HS, Bai Y, Mansell TJ. CRISPR-based curing and analysis of metabolic burden of cryptic plasmids in *Escherichia coli* Nissle 1917. *Eng Life Sci* 2019;**19**:478−85.
41. Zhang H, Lesnov GD, Subach OM, Zhang W, Kuzmicheva TP, Vlaskina AV, et al. Bright and stable monomeric green fluorescent protein derived from StayGold. *Nat Methods* 2024;**21**:657−65.
42. Deng J, Chen Q, Chen Z, Liang K, Gao X, Wang X, et al. The metabolic hormone leptin promotes the function of T(FH) cells and supports vaccine responses. *Nat Commun* 2021;**12**:3073.
43. Castro G, Liu X, Ngo K, De Leon-Tabaldo A, Zhao S, Luna-Roman R, et al. RORgammat and RORalpha signature genes in human Th17 cells. *PLoS One* 2017;**12**:e0181868.
44. Zhu Z, Jin Y, Zhou J, Chen F, Chen M, Gao Z, et al. PD1/PD-L1 blockade in clear cell renal cell carcinoma: mechanistic insights, clinical efficacy, and future perspectives. *Mol Cancer* 2024;**23**:146.
45. Francisco LM, Salinas VH, Brown KE, Vanguri VK, Freeman GJ, Kuchroo VK, et al. PD-L1 regulates the development, maintenance, and function of induced regulatory T cells. *J Exp Med* 2009;**206**:3015−29.
46. Halfvarson J, Brislawn CJ, Lamendella R, Vazquez-Baeza Y, Walters WA, Bramer LM, et al. Dynamics of the human gut microbiome in inflammatory bowel disease. *Nat Microbiol* 2017;**2**:17004.
47. Sultan S, El-Mowafy M, Elgaml A, Ahmed TAE, Hassan H, Mottawea W. Metabolic influences of gut microbiota dysbiosis on inflammatory bowel disease. *Front Physiol* 2021;**12**:715506.
48. Blaak EE, Canfora EE, Theis S, Frost G, Groen AK, Mithieux G, et al. Short chain fatty acids in human gut and metabolic health. *Benef Microbes* 2020;**11**:411−55.
49. Kim CH. Control of lymphocyte functions by gut microbiota-derived short-chain fatty acids. *Cell Mol Immunol* 2021;**18**:1161−71.
50. Han L, Liu XW, Li WX, Zang T, Li ZP, Deng Y, et al. Innovative probiotic *Escherichia coli* nissle 1917-derived outer membrane vesicles coupled microspheres demonstrate anti-inflammatory and barrier-enhancing properties in colitis. *Chem Eng J* 2024;**487**:150711.
51. Li T, Zhu J, Yu Q, Zhu Y, Wu C, Zheng X, et al. Dietary flavonoid quercetin supplement promotes antiviral innate responses against vesicular stomatitis virus infection by reshaping the bacteriome and host metabolome in mice. *Mol Nutr Food Res* 2024;**68**:2300898.
52. Yao Y, Cai X, Fei W, Ye Y, Zhao M, Zheng C. The role of short-chain fatty acids in immunity, inflammation and metabolism. *Crit Rev Food Sci Nutr* 2022;**62**:1−12.
53. van der Hee B, Wells JM. Microbial regulation of host physiology by short-chain fatty acids. *Trends Microbiol* 2021;**29**:700−12.